Conference Paper Manuscript

A Passive System Reliability Analysis for a Station Blackout

prepared by
Acacia Brunett, Matthew Bucknor, David Grabaskas, Tanju Sofu, and Austin Grelle

Nuclear Engineering Division
Argonne National Laboratory
9700 South Cass Avenue, Bldg. 208
Argonne, IL 60439-4854

International Congress on Advances in Nuclear Power Plants 2015
ICAPP 2015
May 03-06, 2015
Nice
France

A Passive System Reliability Analysis for a Station Blackout

Acacia Brunett, Matthew Bucknor, David Grabaskas, Tanju Sofu and Austin Grelle
Argonne National Laboratory, Nuclear Engineering Division
9700 South Cass Ave., Argonne, IL 60439-4854
Tel: (630) 252-7009, Email: abrunett@anl.gov, mbucknor@anl.gov, dgrabaskas@anl.gov, tsofu@anl.gov, agrelle@anl.gov

Abstract – *The latest iterations of advanced reactor designs have included increased reliance on passive safety systems to maintain plant integrity during unplanned sequences. While these systems are advantageous in reducing the reliance on human intervention and availability of power, the phenomenological foundations on which these systems are built require a novel approach to a reliability assessment. Passive systems possess the unique ability to fail functionally without failing physically, a result of their explicit dependency on existing boundary conditions that drive their operating mode and capacity. Argonne National Laboratory is performing ongoing analyses that demonstrate various methodologies for the characterization of passive system reliability within a probabilistic framework. Two reliability analysis techniques are utilized in this work. The first approach, the Reliability Method for Passive Systems, provides a mechanistic technique employing deterministic models and conventional static event trees. The second approach, a simulation-based technique, utilizes discrete dynamic event trees to treat time-dependent phenomena during scenario evolution. For this demonstration analysis, both reliability assessment techniques are used to analyze an extended station blackout in a pool-type sodium fast reactor (SFR) coupled with a reactor cavity cooling system (RCCS). This work demonstrates the entire process of a passive system reliability analysis, including identification of important parameters and failure metrics, treatment of uncertainties and analysis of results.*

I. INTRODUCTION

Advanced reactors maintain many advantages, such as increased plant reliability, modularization, increased power conversion cycle efficiency and reduced capital costs. One of the most prevalent features of advanced reactors is the use of passive safety systems, which generally remove all dependency on human intervention and reliance on power for successful actuation and operation. These unique system characteristics are advantageous in that they reduce system complexity by eliminating nearly all moving components and therefore increase system reliability.

However, incorporating passive system reliability into a probabilistic risk assessment (PRA) can be challenging due to the difficultly in treating the phenomena by which these systems operate. Because passive systems contain no moving parts and rely on no motive force, the mode in which they operate is entirely dependent on the boundary conditions imposed on the system. This unique operating characteristic allows passive systems to fail functionally without failing physically; that is, if the boundary conditions of a passive system deviate sufficiently, the system can fail to provide its safety function without development of any physical component failures in the system. In addition to the unconventional failure modes of passive systems, their performance can be difficult to incorporate into a traditional PRA because of their propensity to operate at intermediate capacities until capacities sufficient to fulfill the safety function have been established. The first-of-a-kind nature of these systems also creates some difficulty in characterization of uncertainties and identification of the operating envelopes of these systems. Until sufficient operating data have been gathered for these systems, the uncertainty in passive system performance may be relatively large.

To address these aforementioned issues, Argonne National Laboratory is currently performing a multi-year demonstration analysis of passive system reliability characterization using various reliability assessment techniques. Previous work at Argonne[1] identified three methods suitable for treatment of passive system reliability: a margins-based approach which characterizes the margin to a conservative failure metric[2], a mechanistic approach similar to a conventional PRA, and a simulation-based method which explicitly considers the time-dependent behavior of the system. The latter two techniques have been identified as promising candidates for performance of a passive system reliability analysis and are explored further in this work.

A metal fuel, pool-type sodium-cooled fast reactor (SFR) has been selected as the advanced, small modular reactor (advSMR) for this demonstration work. The SFR has been paired with a reactor cavity cooling system (RCCS) which relies on natural convection and thermal radiation to cool the reactor cavity. A plant configuration utilizing two passive systems (the primary sodium pool and RCCS) was consciously chosen to examine the feedback effects of coupled passive systems. The plant undergoes an extended station blackout (SBO) with the potential for early to late power recovery, where active heat removal systems may become available if power is reestablished. In these cases, the use of active heat removal systems may create unfavorable criticality conditions in the core due to overcooling by the operation of both active and passive cooling systems. The use of active heat removal systems also has the potential to significantly disrupt passive system behavior such that a functional failure may be induced. All simulations are completed in RELAP5-3D (Ref. 3) deployed on a distributed Windows network under an in-house job server.

The paper structure is as follows: Section II describes the reliability assessment techniques used in this analysis. Section III contains a description of the demonstration problem, including the system model configuration, the top events of the SBO and identification/treatment of uncertainties. The results generated by this analysis are in Section IV, and concluding remarks are in Section V.

II. RELIABILITY ASESSESSMENT TECHNIQUES

A wide range of reliability assessment techniques currently exists for the analysis of passive system reliability. This work utilizes two of the most prevalent methodologies. Mechanistic methods, which are described in Section II.A, are some of the most mature techniques available. Simulation based techniques, which are discussed in Section II.B, offer significant flexibility, but may require additional refinement.

II.A. Mechanistic Methods

Mechanistic techniques are some of the most well-developed and tested methodologies used for the assessment of passive system reliability. The methods range from the Assessment of Passive System Reliability (APSRA) technique, which relies heavily on response surfaces developed from deterministic simulations and experimental data,[4] to other approaches that focus on the uncertainties in the operating envelope of passive systems relative to those of active systems that maintain a significant accumulation of operational data.[5,6]

For this work, the Reliability Method for Passive Systems (RMPS) (Ref. 7) has been selected as the mechanistic technique for passive system reliability assessment. This systematic approach that utilizes deterministic codes and models was initially developed in 2001 by the European Union contracting with the Atomic Energy and Alternative Energies Commission (CEA).[8] The entire methodology contains approximately a dozen discrete steps which involve identification of the system and relevant parameters, screening and quantification of uncertainties, deterministic modeling of the system and quantitative evaluation of the system reliability. For simplicity, the RMPS can be divided into three phases, as shown in Table I. These phases deal with identification and characterization of the system, sensitivity analyses and uncertainty assessment, and incorporation of results into a full PRA.

TABLE I

The Three Phases of the RMPS

Phase 1	• Identify a system, its intended mission, and possible failure modes • Select or develop a best-estimate code to perform the analysis • Identify important system variables, characterize their associated uncertainty
Phase 2	• Conduct sensitivity analysis • Determine failure probability of the system using best-estimate code • Assess the impact of the uncertainties of the important system variable
Phase 3	• Incorporate the failure probability into the PRA

Despite its maturity and robust foundation that is similar to conventional event trees, certain aspects of the RMPS are susceptible to the same limitations of static event trees. The relative ordering and timing of events is required in the RMPS, where the occurrence of phenomena is determined by expert elicitation. In this case, the subjective influence of the analyst/experts on tree development is two-fold, in interpretation of the expert judgment, and in the elicitation itself. Furthermore, reliance on the analyst to describe the accident space via top event specification can lead to omission of important phenomenon that may occur near the boundaries of the accident space. Phenomenological errors can be introduced into the event tree when the full range of uncertainties is explored during the analysis, as the combination of multiple uncertainties can modify the relative timing of events. Explicit treatment of the intermediate operating modes of passive systems can also significantly complicate event tree generation during RMPS. In this case, excessive branching can lead to unmanageable tree growth, making data management difficult, if not impossible.

II.B. Simulation-Based Method

To address some of the limitations of a conventional event tree analysis, simulation-based, or dynamic, techniques have been developed. These methodologies range from discrete dynamic event tree (DDET) software, such as MCDET[9] (which discretizes continuous event trees for practicality), ADS,[10] and ADAPT,[11] to continuous dynamic event tree approaches. The work described in this paper utilizes a simple DDET approach to characterize passive system reliability within a probabilistic framework.

The simulation-based approach shares many common features with a mechanistic technique, such as the use of fault/event trees to describe scenario evolution and quantify the likelihood of end states, and the use of deterministic system codes to model accident progression. However, rather than requiring the pre-specification of event timing, the simulation-based approach allows for the dynamic treatment of phenomena based on the current state of the system. This removes the high level of dependency on the analyst's input to the event tree with regard to event timing and ordering. In this approach, the occurrence of events and progression through accident space is determined by user-defined branching rules with describe the probabilistic behavior as a function of the current state space. Examples of this include the likelihood of creep or pump seal rupture as a function of a cumulative stress function, or the likelihood of hydrogen combustion as a function of the existing combustible gas concentration in a volume and availability of ignition source.

Due to the dependency of passive systems on boundary conditions, DDETs are generally better-suited to treat the reliability of passive systems because of the ability to consider state-dependent failure modes in branching conditions. The lack of moving components in passive systems prevents them from operating in binary states; these systems often require several hours of operation at some intermediate capacity until flow regimes are fully developed. Furthermore, depending on the current status of the plant, operation at some fraction of full capacity could actually be sufficient to fulfill the intended safety function of the passive system. In both cases, conventional event trees with predefined failure criteria would be unable to capture these effects in a risk assessment.

The generation of a DDET is similar to the creation of a conventional event tree. A simulation is launched using a deterministic system level code and proceeds in time until a user-defined branching criteria as a function of state space (e.g. number of valve operations, volume pressure, etc.) is met. At this point, the simulation bifurcates into two parallel sequences: one scenario which includes occurrence of the event (e.g. valve failure, containment rupture, etc.), and one which does not. These two scenarios are then relaunched and run in parallel until another branching condition is met in either scenario. This process repeats until either the mission time is achieved or a failure metric (e.g. core damage) is experienced.

Aleatory and epistemic uncertainties are considered simultaneously in this approach using an inner-outer loop methodology. A single DDET describing the entire aleatory (stochastic) uncertainty space is generated using inner loop iterations. Repetitions of the outer loop generate multiple DDETs and characterize the epistemic uncertainty space that describes the lack of knowledge regarding severe accident phenomenology. Within a family of DDETs created by exploring the epistemic uncertainties, the treatment of stochastic behavior would remain unchanged.

III. DEMONSTRATION PROBLEM

Section III describes the demonstration problem selected for this analysis. Section III.A provides details regarding the coupled SFR-RCCS system model. An overview of the top events considered in this SBO sequence is provided in Section III.B. The process of parameter identification and quantification of relevant uncertainties are described in the final subsection, Section III.C.

III.A. System Model

This work utilizes a relatively simplified SFR design with generic characteristics modeled in RELAP5-3D. Because the objective of this work was to demonstrate various reliability assessment techniques, no effort was made to optimize the plant or use novel design features, and focus was instead placed on the fundamental components of the plant. The pool-type reactor, whose design characteristics are provided in Table II, utilizes metal fuel and operates nominally at 250 MWth. The primary system model contains representation of the core region, outlet/inlet plenums, cold pool, an intermediate heat exchanger (IHX) and four primary electromagnetic (EM) pumps. The primary vessel is surrounded by a guard vessel, where the gap between the two vessels is filled with air. While the IHX is typically used to reject heat to a secondary loop and ultimate heat sink during normal operation, most reactor designs also maintain the ability to utilize the IHX to remove energy from the system via rejection to reduced heat sinks, such as a condenser, while bypassing the power conversion system. A simplified schematic of the primary system with relative component orientations and locations is shown in Figure 1. The nodalization diagram of the primary system for the RELAP5-3D model is shown in Figure 2.

TABLE II

Design Characteristics of the Demonstration SFR

Feature	
Power rating	250 MWth/100MWe
Primary coolant	Sodium
Primary system type	Pool
Fuel type	Metallic
Coolant pump type	Electromagnetic
Coolant pump number	4
Primary vessel height	10 m
Core inlet/outlet temperature	400°C/550°C

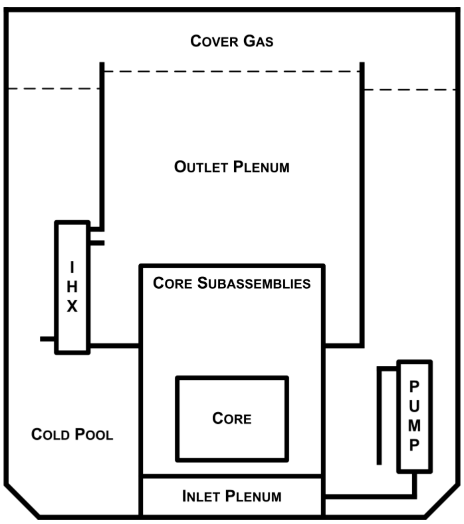

Fig. 1. Simplified schematic of primary system model for demonstration SFR. Orientations and locations are relative, and drawing is not to scale.

With regard to the core model, the existing version of RELAP5-3D utilizes a point reactor kinetics model that explicitly considers separable feedback effects in the moderator and fuel, where only material densities and temperatures in these regions are considered when determining feedback effects. This type of reactivity feedback treatment is sufficient for oxide fuel light water reactors, but metal fuel, liquid metal cooled reactors experience significant feedback from radial expansion of the core and elongation of the reactor vessel and control rod drivelines. For this reason, an alternative treatment of the core and the associated reactor kinetics was required. To input fission power during unprotected scenarios where the reactor does not scram, an integral solution to the space-averaged reactor kinetics equation[12] was implemented using the control structure scheme in RELAP5-3D. Temperature-dependent feedback due to radial expansion, Doppler broadening, and control rod driveline expansion/vessel elongation are the dominant mechanisms considered in the feedback model. For scenarios in which the reactor does scram successfully, a programmed reactivity component is supplied to RELAP5-3D, where the time-dependent curve has been derived from SAS4A/SASSYS-1 (Ref. 13) analyses for a similar reactor and scenario. The decay heat component of reactor power for protected and unprotected scenarios was also derived from SAS4A/SASSYS-1 analyses for a similar facility and scenario.

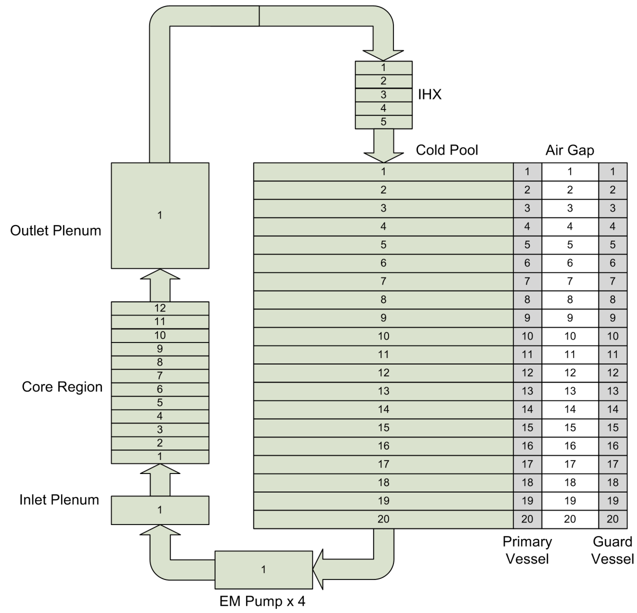

Fig. 2. Nodalization diagram of the RELAP5-3D demonstration SFR model. Node sizes and pipe lengths are not to scale.

For this work, the primary system has been paired with the RCCS, which passively cools the reactor cavity via a combination of natural convection and thermal radiation. Typical SFR designs are paired with a system similar to a reactor vessel auxiliary cooling system, however, the RCCS was included in this analysis due to the availability of the Natural convection Shutdown heat removal Test Facility (NSTF) at Argonne. A recently constructed experimental facility, the NSTF is a half-scale representation of the RCCS. Experiments completed during FY14 have been utilized to complete benchmarking of the RCCS RELAP5-3D model as part of this work.[14]

Originally designed by General Atomics for inclusion in the Modular High Temperature Gas cooled Reactor (GA-MHTGR),[15] the RCCS relies on natural convection and thermal radiation to remove decay heat from the primary system and reactor cavity via a series of hot riser tubes located within the reactor cavity. Cooling air from the atmosphere enters the system by means of a downcomer; this air then travels through hot riser tubes and out a series of chimneys, which vent to the atmosphere. The RCCS contains no baffles or dampers, and is therefore removing energy from the system during normal operation. A plan view of the RCCS within the cavity is shown in Figure 3, and the overall system layout is shown in Figure 4.

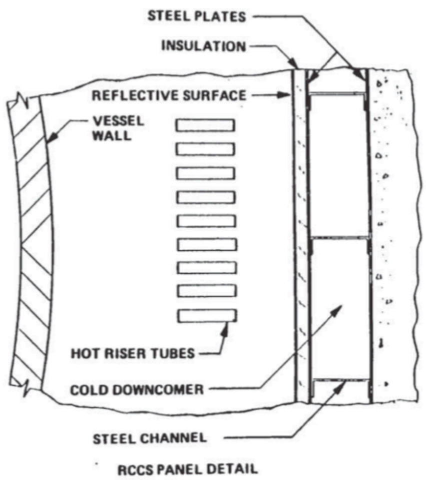

Fig. 3. Plan view of the RCCS showing the hot riser tubes within the cavity.[15]

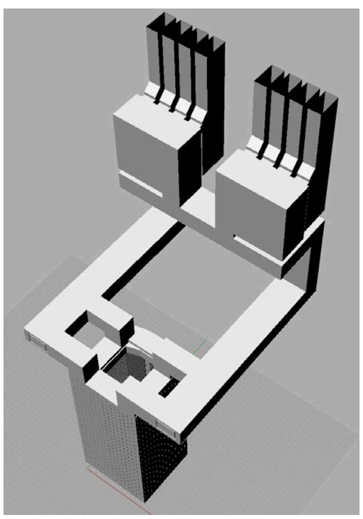

Fig. 4. System level view of the RCCS, showing the cavity enclosure and chimneys.[16]

III.B. Scenario Description

The importance of properly capturing passive system performance is not necessarily evident in all accident scenarios since the demand on the passive system varies depending on the accident scenario. A prolonged, grid-induced station blackout (SBO) was selected for this work because it is an ideal scenario for demonstrating the coupled feedback effects between the RCCS and primary system. Additionally, it is expected that SBOs will receive additional regulatory attention due to the events at Fukushima in 2011.

A simplified SBO event tree containing a limited set of top events is utilized in this work, where this event tree is based on the SBO event tree for GE's SFR design, PRISM.[17] Only events expected to have a significant influence on the performance of the passive systems were included in the event tree. Table III shows the top events considered in this analysis, the associated probabilities and sources, where applicable.

The SBO initiating event (IE) produces a complete loss of power at the plant, where it is assumed that a massive grid-induced disruption produces the prolonged loss of power. As is common in some SFR designs,[17] onsite safety grade diesel generators are not included in the plant design; therefore the recovery of onsite power via diesel generator restoration is not considered in this work. The likelihood of this event is taken from a 2005 assessment by the U.S. NRC of the current risk of SBOs at U.S. commercial nuclear installations.[18] Successful reactor shutdown following the IE requires the reactor protection system (RPS) to successfully send a scram signal to the reactor shutdown system (RSS) and for a sufficient number of control rods to be inserted. The PRISM PSID determined that one fully inserted control rod was sufficient to shutdown the reactor. However, in an effort to simplify the kinetics model, it is assumed that either all or no control rods are inserted resulting in a protected or unprotected sequence, respectively.

Pump coastdown failure is treated with a higher level of detail relative to the other top events as it introduces varying power to flow ratios during the initial stages of the accident. In the absence of mechanical impellers to provide inertial force, EM pumps require a separate flywheel and synchronous machine to simulate the gradual reduction in flow rate experienced by mechanically-impelled pumps. In the event of coastdown failure, coolant flow ceases nearly instantaneously and the coolant temperature increases rapidly in the core region. The likeliehood of failure of a single pump to coastdown properly is derived from the PRISM PSID. Failure of multiple coastdown mechanisms is assumed to occur due to common cause failure (CCF), where the likelihoods were calculated using an alpha factor model with staggered testing.[20]

As a consequence of the structure of the IE, several top events in Table III have probabilities of unity. Primary pumps and operating power heat removal both require offsite power to operate successfully; therefore, these systems will be unavailable immediately following the IE. As part of this analysis, the RCCS is assumed to operate successfully without any probability of failure or consideration of degradation. Future analyses in FY15 will consider degraded operating states of the RCCS.

The final top event in Table III represents the sampling of all uncertain parameters and indicates the final end state of the facility. This event allows for the explicit consideration within the event tree of uncertainty propagation through the entire model. The likelihood of this branch is determined by the fraction of scenarios that experience the damage criteria and are considered to be in a failed state. Direct utilization of risk results has similarly been applied by a Risk Informed Safety Margin Characterization (RISMC) of a total loss of feedwater event.[21] Additional details regarding uncertainty sampling is included in Section III.C.

TABLE III

Top Events Considered in the SBO Analysis

Top Event	Probability	Source/Comment
SBO (IE)	9.19E-2 per ry	95^{th} percentile from Ref. 18
RPS Signal to RSS	P(fail) = 2.4E-5	Ref. 17 and 19
Enough Control Rods Inserted	P(fail) = 5.8E-5	Ref. 17 and 19
Pump Trip	P(trip) = 1.0	All EM pumps trip due to SBO IE
Pump Coastdown	P(1/4 fail) = 5.0E-5 P(2/4 fail) = 1.63E-6 P(3/4 fail) = 5.54E-7 P(4/4 fail) = 4.21E-7	Single failure probability from Ref. 17; Alpha factor model with staggered testing for CCF[20] used to determine remaining probabilities
Operating Power Heat Removal	P(fail) = 1.0	All active systems fail due to SBO IE
RCCS Operating	P(operating) = 1.0	Assume RCCS intact and functioning for FY14 analyses
Delayed Active Heat Removal	P(power recovery time) = U[4.0,24.0] P(power recovery within 24 hr following IE) = 0.5 *Mechanistic:* - Dependent exclusively on power recovery *Simulation-based:* - Dependent on power recovery and primary system temperature	See Sections III.B.1 and III.B.2 for discussion of mechanistic and simulation-based approach to active decay heat removal, respectively
Sampling	Determined by sampling from uncertain parameters; Sampled values fed directly into model input	See Section III.C

*IE = initiating event, RPS = reactor protection system, RSS = reactor shutdown system

III.B.1 Mechanistic Approach to Power Recovery and Active Heat Removal

In the mechanistic approach, the actuation of delayed active heat removal is entirely dependent on the timing of offsite power recovery. Because this analysis is intended to serve as a methodology demonstration, the method of power recovery (e.g. use of portable equipment, grid reconnection, etc.) was not explicitly treated in this work and it is instead assumed that power recovery is equally likely between 4 hr and 24 hr following the IE. To control tree growth and simplify the analysis, power recovery is only considered at 9 hr and 19 hr following the IE in an effort to concisely represent the entire timeframe of interest. If power is recovered, it is assumed that active heat removal will be utilized immediately.

For this work, it is conservatively assumed that power is not recovered within 24 hr with a likelihood of 0.5. Accordingly, the likelihood of power recovery at 9 hr and 19 hr is 0.25 at each branch. These power recovery options and associated probabilities are shown in Table IV. It should be noted that the probability of some degree of power recovery within 24 hr is likely to be fairly high now given post-Fukushima coping requirements.

TABLE IV

Power Recovery Options for Mechanistic Analysis

Option	Probability	Comment
No recovery within 24 hr	P(no recovery) = 0.5	Assumed equipment and staff unavailable
Early recovery (9 hr after IE)	P(recovery) = 0.25	Represents first half of timeframe
Late recovery (19 hr after IE)	P(recovery) = 0.25	Represents latter half of timeframe

III.B.2 Simulation-Based Approach to Power Recovery and Active Heat Removal

Similar to the mechanistic analysis, the simulation-based approach assumes that power recovery is equally likely (i.e. uniformly distributed) between 4 hr and 24 hr following the IE. However, where the mechanistic approach considered power recovery either early or late in the scenario, the simulation-based analysis questions power recovery at four hour intervals following the IE. As with the mechanistic analysis, the likelihood of non-recovery within 24 hr is assumed to be 0.5. A graphical depiction of the power recovery options and the likelihood of each branch is shown in Fig. 5. It should be noted that this power recovery tree does not include the likelihood of active heat removal actuation, and is only representative of the assumed likelihood of power recovery. Each event tree considers all of the power recovery options described in Fig. 5.

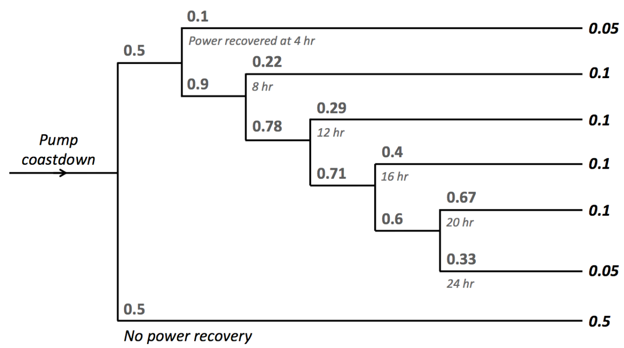

Fig. 5. Power recovery options and associated probabilities for the simulation-based analysis.

Where the mechanistic approach assumed only power recovery was required for active heat removal actuation, the simulation-based analysis also checks the status of the primary system before utilizing active heat removal systems. In a real plant, guidelines may discourage the simultaneous use of active and passive systems as this creates an opportunity to overcool the system and introduce positive reactivity. However, if the passive system is not removing an adequate quantity of heat from the primary system, use of the active heat removal system may be required to maintain component or core integrity. Decision-making logic has been implemented in the RELAP5-3D model which will only allow use of active heat removal if the primary bulk sodium temperature is above 600°C and power has been recovered. A decision tree showing this logic is depicted in Fig. 6.

This threshold is not intended to prevent sodium boiling, but instead has been selected to satisfy the ASME boiler and pressure vessel service limits which delineate loading limits on reactor grade materials.[17,22] The service limits describe inspection requirements that are dependent on the integral stress a component experiences. In more severe cases with elevated temperatures, use or operation of the component may not be possible as per the ASME code. In these cases, the decision to utilize active systems would be motivated by the potential economic consequences before any concerns of core integrity developed.

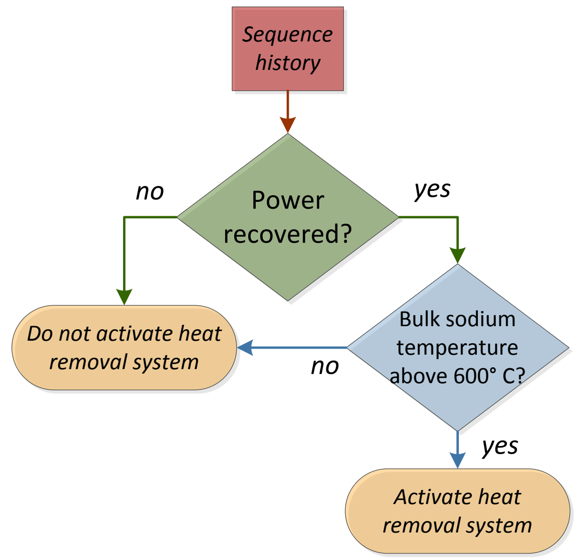

Fig. 6. Decision-making logic utilized to determine if active heat removal will be actuated in simulation-based approach.

III.C. Parameter Identification, Sensitivity Analysis and Screening, and Uncertainty Quantification

The identification, screening and quantification of important parameters and uncertainties is a nontrivial component of a risk assessment. Insufficient identification of influential parameters can lead to omission of important phenomena and regions of the accident space, but over-characterization of important parameters can significantly burden the analysis by creating unnecessarily large event trees. For meaningful results regarding passive safety system performance, the parameters that are expected to have a significant effect on system performance must be included. In an effort to simplify the demonstration problem, a fairly limited set of uncertainties is used in this work, where the majority of the selected parameters relate to the performance of RCCS. Uncertainties affecting heat levels in the primary system have also been selected for consideration.

The important parameters and the quantification of their uncertainties are provided in Table V. The majority of the distributions have been derived from engineering judgment and the PRISM PSID. As shown in Table V, in the absence of actual component and material specifications, it is assumed that most of the uncertainties are normally distributed.

TABLE V

Important Parameters and Quantified Uncertainties

Parameter	**Characterization**
Ambient temperature	*U*(-30.0,45.0)
Primary vessel emissivity	*N*(0.77,0.35)
Primary vessel thermal conductivity	*N*(1.0,0.0125)
Guard vessel emissivity	*N*(0.77,0.35)
Guard vessel thermal conductivity	*N*(1.0,0.0125)
Hot riser tubes emissivity	*N*(0.77,0.35)
Hot riser tubes thermal conductivity	*N*(1.0,0.0125)
Steel liner emissivity	*N*(0.77,0.35)
Duct surface roughness	ln*N*(3.45,0.70)
Initial power level	*N*(1.0,0.025)
Decay heat curve	*N*(1.0,0.025)

In Table V, the material properties of the primary and guard vessels, hot riser ducts and steel liner were chosen as important uncertainties as they are expected to significantly affect heat rejection from the primary system and RCCS. The distribution characterizing the primary vessel, guard vessel and hot riser tube emissivities was derived from the PRISM PSID, where the conservative value reported in the PSID was assumed to be the 95th percentile value. The thermal conductivities, applied as a scaling factor to the existing RELAP5-3D correlation, are assumed to vary by up to 2.5% of its mean value; the relatively small uncertainty bands are expected to be the result of manufacturing inconsistencies rather than material degradation over the lifetime of the facility. Significant variation in duct surface roughness is assumed to occur over the lifetime of facility due to the cyclical accumulation and removal of particulate and debris. Values of 10 μm and 100 μm were chosen as the 5th and 95th percentiles, respectively, of the lognormal distribution representing surface roughness. The ambient air temperature was also selected as an important parameter that may significantly affect RCCS performance. Conservative values representing seasonal changes in a non-specific climate were chosen to explore this uncertainty. It is assumed that the ambient air temperature varies uniformly between -30°C and 45°C. Uncertainties expected to have a significant effect on heat level in the primary system include the initial power level and the decay heat curve. Both of these parameters are applied as scaling factors to the existing curves and correlations in RELAP5-3D. These parameters are assumed to vary by up to 5% of their mean values.

Sensitivity analyses completed for this work primarily explored the modeling uncertainties in and capabilities of RELAP5-3D. This included validation of the sodium property library via stand-alone calculations, and preliminary analyses of thermal stratification in the cold pool. Early attempts to explicitly treat stratification led to model instability, so the final model utilizes a thermally well-mixed volume, which is consistent with the approach utilized by most SAS4A/SASSYS-1 primary models.

Screening of the selected parameters was accomplished by performing a Failure Modes and Effects Analysis (FMEA) and Hazards and Operability Study (HAZOP) for the RCCS.[23] Key performance characteristics of the RCCS were addressed in this analysis, including the flow rate, pressure and heat transfer capability of various components of the system. The parameters identified in Table V were identified as part of the FMEA and HAZOP. However, other factors identified in the FMEA and HAZOP, such as RCCS sump and flow blockage, were not included in this analysis as they were outside the scope of this FY14 analysis.

Early reactivity modeling efforts also included all conventional forms of reactivity feedback mechanisms, including material and geometry changes. Screening analyses showed that structural and axial feedback were negligible relative to other mechanisms, and were therefore removed to simplify the control structure logic in RELAP5-3D.

IV. RESULTS

This section describes the results of this demonstration problem. Section IV.A outlines the solution methodology. The core damage metrics utilized are discussed in Section IV.B. The numerical results and accompanying discussion are in Sections IV.C and IV.D for the mechanistic and simulation-based approaches, respectively. Section IV.E compares the results obtained using each methodology and provides comments on the strengths and weaknesses of each approach.

IV.A. Solution Methodology

To perform simulations and generate the event trees, a straightforward solution methodology was implemented. Monte Carlo samples were drawn from the uncertainty distributions shown in Table V; the selected values were then inserted into the RELAP5-3D input deck containing the decision-making and/or branching rules described in III.B, and the simulation was executed accordingly. The simulation continues until a specific branching condition or top event is met, at which point the simulation will halt, and two parallel scenarios with alternative branches are generated and executed. This entire process generates a single event tree. To generate a second event tree, an additional set of samples is drawn, inserted into the input deck, and the deck is launched. For both the mechanistic and simulation-based approaches, a total of 100 samples were drawn from each uncertainty distribution, thereby generating 100 complete, unique event trees for each technique.

All simulations were executed on a distributed Windows network under an in-house job server. Scenarios were executed until either a core damage metric (see Section IV.B) was met, or until the simulation reached its mission time of 72 hr. A core damage probability was determined for each tree, and a cumulative core damage frequency that considers all trees was found. Results for this analysis are presented both with and without a 95% confidence interval to assess the adequacy of the sample size.

IV.B. Core Damage Metrics

Because a simplified core model was implemented in RELAP5-3D as part of this analysis, core damage could not explicitly be modeled and tracked. Instead, surrogate core damage metrics were utilized that track the likelihood of core damage as a function of peak clad and sodium temperature in the core region. The coolant temperature was tracked as a binary sodium boiling indicator. Conventionally, sodium boiling, which occurs at 883°C at 1 atm., is considered a core damage metric in SFR safety analyses as it is assumed that localized fuel damage will occur in the voided regions due to the reduced heat transfer. Beyond this phenomenological assumption, some modeling limitations exist above the sodium temperature, as most system level codes do not maintain well-implemented sodium properties and phenomenological models above this temperature.

Peak cladding temperature was also used as a core damage metric to represent the eutectic penetration phenomenon. Metal fuel degradation is highly dependent on the formation of a eutectic, or a mixture of multiple materials that possesses a lower melting point than any of its constituents. The formation of a eutectic is strongly dependent on time at temperature; at 650°C, metal fuel failure occurs after several hundreds of hours, whereas at temperatures near the boiling point of sodium, failure can occur on the order of minutes.[24] While it is evident that a cumulative damage function is necessary to accurately model eutectic formation and penetration, development and implementation of such a correlation was beyond the scope of this work. Instead a one-sided normal distribution describing the probability of failure as a function of clad temperature was developed for this work. Under this distribution, at temperatures below 700°C, the likelihood of failure approach zero; as the clad temperature approaches the sodium boiling temperature of 883°C, the likelihood of failure goes to 0.5. Because metal fuel has enhanced heat transfer characteristics, the clad temperature tracks very closely with the coolant temperature; therefore, the failure likelihood goes to 1.0 at 883°C due to the sodium boiling metric. The distribution describing failure as a function of peak clad temperature is shown in Fig. 7.

It should be noted that the core damage metrics used in this analysis are considered very conservative, particularly when applied in conjunction with one another. It is unlikely that localized failures in the clad will lead to large releases resulting in any measureable offsite consequences. Additionally, core damage in SFRs is not well-defined. For most pool-type designs, it is expected that localized clad damage will allow for ejection of molten fuel into the primary coolant, where it will be swept out of the core region and effectively lead to core shutdown. Accounting for this phenomenon, however, is beyond the scope of this work, as a detailed core model would be required.

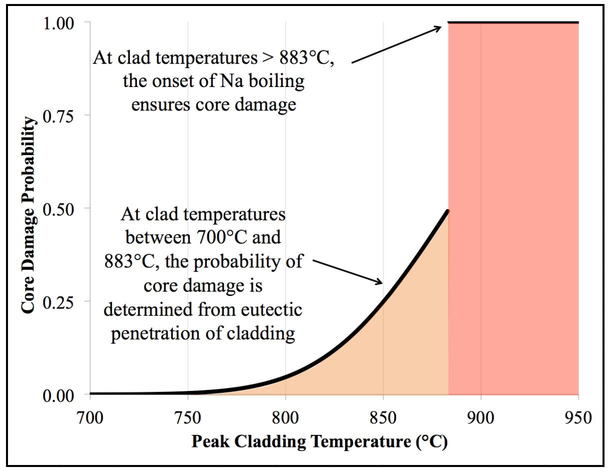

Fig. 7. Distribution describing the likelihood of core damage as a function of peak clad temperature. Between 700°C and 883°C, the likelihood is dominated by eutectic formation, whereas at 883°C at higher, it is conservatively assumed sodium boiling guarantees core damage.

IV.C. Mechanistic Results

The core damage frequency determined from the mechanistic analysis is shown in Table VI. Results are presented using the sodium boiling indicator combined with the eutectic penetration distribution, and for the sodium boiling indicator only so that the effect of the simplified eutectic model can be assessed. Results are also presented with and without the 95% confidence interval (CI).

TABLE VI

Final Results of the Mechanistic Analysis

Core Damage Metric	**Core Damage Frequency (yr^{-1})**	**Core Damage Frequency w/ 95% CI (yr^{-1})**
Sodium boiling and eutectic penetration	1.337E-6	1.347E-6
Sodium boiling only	2.189E-12	2.432E-12

Table VI shows that the core damage frequency is strongly affected by the core damage metric, as results using only the sodium boiling indicator are six orders of magnitude lower relative to results that include the eutectic penetration model. This significant difference is largely due to the number of scenarios that experience sodium boiling relative to the number of scenarios that only experience elevated temperatures below the boiling point of sodium. Sodium boiling only occurs in some fraction of scenarios that experience scram failure and coastdown failure in all four EM pumps. There is a significant increase in core damage frequency when the eutectic penetration model is included because nearly all unprotected scenarios experience temperatures above 700°C, which is effectively the threshold for core damage in the simplified eutectic model. Approximately two-thirds of scenarios in each tree result in unprotected transients, where the failure likelihood of the RPS required to shutdown the core is on the order of 1.0E-5.

The results in Table VI also indicate that the sample size of 100 event trees is adequate, as there is little variance in the core damage frequency when the 95% confidence interval is applied. A relatively larger difference can be seen when the confidence interval is applied to the sodium boiling only metric. As a binary indicator, the sodium boiling metric is expected to have a relatively higher variance.

IV.D. Simulation-Based Results

Numerical results of the simulation-based approach are shown in Table VII. As with the mechanistic results, the core damage frequency has been calculated using the sodium boiling and eutectic penetration model, and the sodium boiling only indicator. Results are also shown with and without the 95% confidence interval.

TABLE VII

Final Results of the Simulation-Based Analysis

Core Damage Metric	**Core Damage Frequency (yr^{-1})**	**Core Damage Frequency w/ 95% CI (yr^{-1})**
Sodium boiling and eutectic penetration	1.508E-6	1.556E-6
Sodium boiling only	2.189E-12	2.432E-12

Similar to the mechanistic results, the core damage frequency is six orders of magnitude smaller when the sodium boiling only metric is utilized. This is due to the number of scenarios experiencing sodium boiling relative to the number of scenarios that experience temperatures of 700°C or greater. In the simulation-based approach, sodium boiling only occurs in unprotected scenarios with coastdown failure in all four EM pumps, which is a fairly small subset of scenarios. Approximately two-thirds of all scenarios incur temperatures above 700°C as the result of the failure to scram the reactor, where the failure likelihood of the RPS which is required for reactor scram is on the order of 1.0E-5.

Application of the 95% confidence interval again indicates that the sample size is adequate. The results in Table VII show little variance in results with and without the 95% confidence interval. Typical with all binary indicators, a slightly larger variance is observed in the sodium boiling only metric.

IV.E. Comments and Comparison of Methodologies

One of the most important observations derived from this analysis is the importance of mechanistically capturing the feedback effects between coupled passive systems. This is most evident in unprotected cases with power recovery in the simulation-based approach. Figures 8 and 9 show results from five Monte Carlo samples (event trees) in the simulation-based analysis with power recovery at 4 hr and 8 hr. It should first be noted that in nearly all unprotected scenarios, the bulk sodium temperature increases beyond 600°C within 11 hr, therefore, the only variability in active heat removal actuation times in the simulation-based approach occurs in cases with power recovery at 4 hr and 8 hr and these are therefore the only results shown for clarity.

The effect of core temperature and active heat removal actuation on reactor power in unprotected transients is shown in Fig. 8, which shows core outlet temperature (dashed lines) and core power (solid lines) as a function of time. In the first few hours of the scenarios, the increasing core outlet temperature leads to a reduction in core power due to the negative feedback characteristics of metal fuel. Upon its actuation, active heat removal quickly reduces the primary coolant temperature, however there is a delayed effect on core power that is the result of the gradual reduction of negative reactivity in the core. Approximately an hour after the actuation of active heat removal systems, the core becomes critical and power increases once sufficient negative reactivity has been removed from the system. The core outlet temperature goes to a new equilibrium value approximately four hours after the actuation of active heat removal, with core power also going to a new steady state value within several hours.

Figure 9 shows the effect of the primary system heat level on the performance of the RCCS. In this figure, which corresponds to the data shown in Figure 8, it can be seen that the mass flow rate through the RCCS is directly coupled with the core outlet temperature. Immediately upon actuation of primary system cooling, flow through the RCCS is disrupted and decreases for several hours. Approximately ten hours are required for the RCCS to achieve a new equilibrium flow rate.

The core outlet temperature and power curves shown in Fig. 8 indicate some degree of clustering; this behavior is the result of the discrete power recovery times. The first four curves of each data channel correspond to scenarios with power recovery at 4 hr. The remaining curves, which are more closely clustered, correspond to scenarios with power recovery at 8 hr. The large gradient in the results of scenarios with power recovery at 4 hr indicates that epistemic uncertainties are more influential in early scenario behavior when the transient is rapidly evolving.

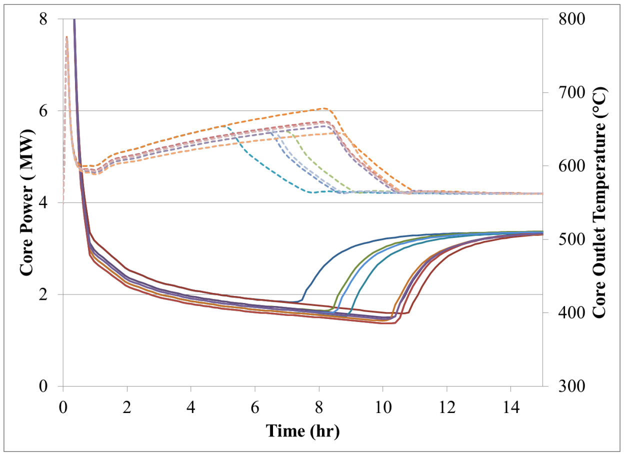

Fig. 8. Core power (solid) and outlet temperature (dashed) for unprotected scenarios with power recovery at 4 hr and 8 hr from the simulation-based approach. Scenarios with no power recovery are not shown.

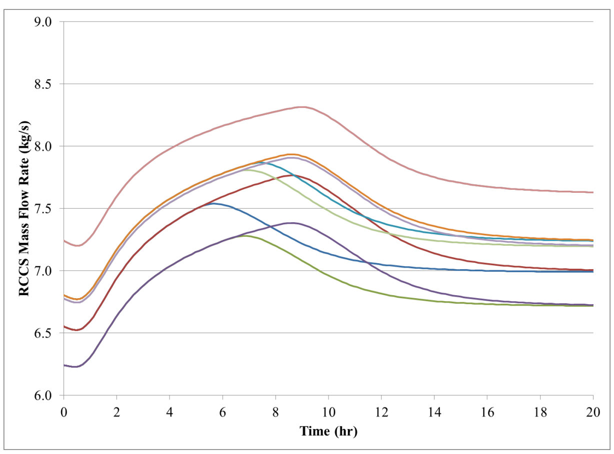

Fig. 9. Mass flow rate of air through the RCCS for unprotected scenarios with power recovery at 4 hr and 8 hr from the simulation-based approach. These scenarios correspond to those shown in Fig. 8.

This analysis also demonstrated the ability of the simulation-based approach to efficiently capture dynamic phenomena and model behavior and also emphasized the importance of capturing the influence of uncertainties on accident progression. Figures 8 and 10 show analogous results (the coupled behavior of core power and outlet temperature) produced with the simulation-based approach and mechanistic technique, respectively. The simulation-based analysis (Fig. 8), where active heat removal was dependent on power recovery and the status of the primary system, produces a continuous range of curves, indicating that inclusion of uncertainties can introduce a significant variation in system behavior. This type of behavior can easily be missed in a mechanistic analysis (Fig. 10) which produces discretized results with power recovery times at 9 hr and 19 hr. If a higher resolution of active removal actuation times was desired in the mechanistic analysis, a substantial number of branches would need to be added to the event tree which would ultimately make it unmanageable.

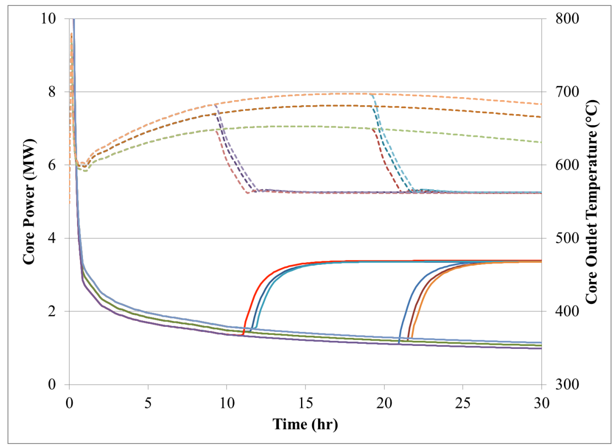

Fig. 10. Core power (solid) and outlet temperature (dashed) for unprotected scenarios from the mechanistic analysis. Results are shown for scenarios with power recovery at 9 hr and 19 hr, and no power recovery from three event trees.

The importance of capturing the effects of uncertainties can also be demonstrated by correlation analyses. The correlation between sodium boiling and each uncertain parameter has been determined using the Pearson product-moment correlation coefficient and is provided in Table VIII for unprotected cases with pump coastdown failure in all four primary pumps. In Table VIII, ±1 indicates perfect correlation (positive or negative), and 0 indicates no relationship. The results show that uncertainties affecting primary heat levels at the onset of the accident, such as the initial power level and the decay heat curve, have the greatest correlation with sodium boiling. Thermal conductivities in the primary vessel and hot riser tubes are also important relative to other uncertain parameters. Due to the generic problem design for this demonstration analysis, the Pearson coefficients have a somewhat limited value in this application. However, in a true risk assessment, a vendor or utility could ascertain which systems or components have the greatest influence and target these areas for the most cost-effective improvements in plant safety and system performance. Correlation results can also be used to check for unintuitive system behavior. For the results shown in Table VIII, sodium boiling and scenario failure occur fairly shortly after the IE, so it would be expected that primary heat levels, which have rapid effects early in the transient, show the strongest correlation with sodium boiling.

TABLE VIII

The Pearson Coefficient for Sodium Boiling

Parameter	Pearson Coefficient
Ambient temperature	-0.094
Primary vessel emissivity	-0.178
Primary vessel thermal conductivity	-0.206
Guard vessel emissivity	-0.055
Guard vessel thermal conductivity	-0.047
Hot riser tubes emissivity	0.117
Hot riser tubes thermal conductivity	0.224
Steel liner emissivity	-0.064
Duct surface roughness	-0.106
Initial power level	0.486
Decay heat curve	0.558

V. CONCLUSIONS

This work demonstrated two feasible techniques for the analysis of passive system reliability within a probabilistic framework. Even though each analysis is built upon a unique foundation, both techniques share common elements that are fundamental components of the reliability assessment. In both approaches, the importance of model development, parameter identification and uncertainty quantification are evident. However, each methodology presents unique strengths. Uncertainty correlation and analysis of high-impact parameters is more straightforward in the mechanistic approach due to the rigidity of the event tree. The simulation-based approach, however, outperformed the mechanistic event trees in capturing dynamic system behavior, which can become important when considering the full range of uncertainties. Both techniques demonstrated the importance of utilizing a coupled mechanistic model of the facility and the importance of capturing the effects of uncertainties via system simulation. While different numerical results for the cumulative core damage frequency were produced, this does not imply that one technique is more statistically correct. The deviation in results is produced by the inclusion of the decision-making logic model and addition of power recovery times to the simulation-based approach.

This demonstration analysis contains analysis components that may satisfy future regulatory requirements; as advanced reactors enter the licensing phase, it is increasingly important for vendors to consider the regulatory perspective of reactor safety. The recently issued ASME/ANS PRA standard for Advanced Non-Light Water Reactors[25] imposes certain requirements on mechanistic modeling of passive systems, where empirical models and correlations are required to treat passive system performance. Additionally, some level of uncertainty identification and quantification is required, where the maturity of the reactor design and intent of the safety analysis directly affects the required treatment of uncertainties.

It is important to stress that the numerical results of this analysis have been derived using several very conservative assumptions and model simplifications. The use of sodium boiling and a simple eutectic penetration model as a core damage metric is not conventional; additionally, the eutectic penetration correlation was simplified in its assumptions and limited in its capability due to the coarse core model. The primary system model was fairly simplified relative to the higher-fidelity RCCS model, which prevented inclusion of some important primary system parameters that may have affected accident progression. Ultimately, the level of model fidelity will need to be determined by the intended purpose of the analysis.

It should also be noted that this analysis is not a commentary on the viability of coupling a pool-type SFR with a passive system such as the RCCS. The intent of this work was to demonstrate the inclusion of passive systems in a probabilistic risk assessment and to emphasize the important components of such an analysis. While this analysis assumed the RCCS was fully functional, future work will examine the effects of reduced RCCS capabilities on the state of the plant.

ACKNOWLEDGMENTS

Argonne National Laboratory's work was supported by the U.S. Department of Energy, Assistant Secretary for Nuclear Energy, Office of Nuclear Energy, under contract DE-AC02-06CH11357.

REFERENCES

1. D. GRABASKAS, and T. Sofu, "Review of Passive System Reliability Modeling Approaches for Advanced Small Modular Reactors," *Proceedings of ANS PSA 2013 International Topical Meeting on Probabilistic Safety Assessment and Analysis,* Columbia, SC, Sept. 22-26, American Nuclear Society (2013).

2. N.S. SALTOS, A. El-Bassioni, and C.P. Tzanos, "A Risk-Based Margins Approach for Passive System Performance Reliability Analysis," *Progress in Design, Research, and Development and Testing of Safety Systems for Advanced Water Cooled Reactors: Proceedings of a Technical Committee Meeting*, Piacenza, Italy (1995).

3. The RELAP5-3D Code Development Team, "RELAP5-3D Code Manual," INEEL-EXT-98-00834, Rev. 4, Idaho National Laboratory, Idaho Falls, ID (2012).

4. A.K. NAYAK, M.R. Gartia, A. Antony, G. Vinod, and R.K. Sinha, “Passive System Reliability Using the APSRA Methodology,” *Nuclear Engineering and Design*, **238**, pp. 1430-1440 (2008).

5. F. MACKAY, G. Apostolakis, and P. Hejzlar, “Incorporating Reliability Analysis Into the Design of Passive Cooling Systems with an Application to a Gas-cooled Reactor,” *Nuclear Engineering and Design*, **238**, pp. 217-228 (2008).

6. C.J. FONG, and G. Apostolakis, “The Use of Response Surface Methodology to Perform Uncertainty Analyses on Passive Safety System,” *PSA ’08, International Topical Meeting on Probabilistic Safety Assessment,* Knoxville, TN, Sept. 7-11, American Nuclear Society (2008).

7. M. MARQUES, et al., “Methodology for the Reliability Evaluation of a Passive System and its Integration into a Probabilistic Safety Assessment,” *Nuclear Engineering and Design,* **235**, pp. 2612-2631 (2005).

8. EUROPEAN COMMISSION, “RMPS Project: Reliability Methods for Passive Systems,” 5th Euratom Framework Programme 1998-2002.

9. M. KLOOS, and J. Peschke, “MCDET: A Probabilistic Dynamics Method Combining Monte Carlo Simulation with the Discrete Dynamic Event Tree Approach,” *Nuclear Science and Engineering*, **153**, pp. 137-156 (2006).

10. K. HSUEH, and A. Mosleh, “The Development and Application of the Accident Dynamic Simulator for Dynamic Probabilistic Risk Assessment of Nuclear Power Plants,” *Reliability Engineering and System Safety*, **52**, pp. 279-296 (1996).

11. A. HAKOBYAN, et al., “Dynamic Generation of Accident Progression Event Trees,” *Nuclear Engineering and Design*, **238**, 3457-3467 (2008).

12. G.R. KEEPIN, *Physics of Nuclear Kinetics,* Addison-Wesley Publishing Company, Reading, Mass. (1965).

13. Editor: T.H. FANNING, “The SAS4A/SASSYS-1 Safety Analysis Code System: User’s Guide,” ANL/NE-12/4, Argonne National Laboratory, Argonne, IL (2012).

14. D. GRABASKAS, M. Bucknor, A. Brunett, T. Sofu and A. Grelle, Argonne National Laboratory, unpublished information (2014).

15. U.S. DEPARTMENT OF ENERGY, “Preliminary Safety Information Document for the Standard MHTGR,” HTGR-86-024, Vol. 1, Amendment 13 (1992).

16. S. LOMPERSKI, D.W. Pointer, C.P. Tzanos, T.Y.C. Wei and A. Kraus, “Air-Cooled Option RCCS Studies and NSTF Preparation,” ANL-GenIV-179, Argonne National Laboratory, Argonne, IL (2011).

17. GENERAL ELECTRIC, “PRISM Preliminary Safety Information Document,” GEFR-00793, UC-87Ta, San Jose, CA (1987).

18. U.S. NUCLEAR REGULATORY COMMISSION, “Reevaluation of Station Blackout Risk at Nuclear Power Plants,” NUREG/CR-6890, Washington, D.C. (2005).

19. U.S. NUCLEAR REGULATORY COMMISSION, “Preaaplication Safety Evaluation Report for the Power Reactor Innovative Small Module (PRISM),” NUREG-1368, Washington, D.C. (1994).

20. U.S. NUCLEAR REGULATORY COMMISSION, “Guidelines on Modeling Common-Cause Failures in Probabilistic Risk Assessment,” NUREG/CR-5485, Washington, D.C. (1998).

21. C. SMITH, C. Rabiti and R. Martineau, “Risk Informed Safety Margin Characterization (RISMC) Pathway Technical Program Plan,” INL/EXT-11-22977, Idaho National Laboratory, Idaho Falls, ID (2013).

22. AMERICAN SOCIETY OF MECHANICAL ENGINEERS, “ASME Boiler and Pressure Vessel Code, Section III, Division 5, High Temperature Reactors: Rules for Construction of Nuclear Facility Components,” 2010 Edition, New York, NY (2010).

23. CHEMICAL INDUSTRIES ASSOCIATION, CHEMICAL INDUSTRY SAFETY AND HEALTH COUNCIL, “A Guide to Hazard and Operability Studies,” U.S. Chemical Industry Safety and Health Council of the Chemical Industries Association (1977).

24. M. DENMAN, “Probabilistic Transient Analyses of Fuel Choices for Sodium Fast Reactors,” Dissertation, Massachusetts Institute of Technology (2011).

25. AMERICAN SOCIETY OF MECHANICAL ENGINEERS, “Probabilistic Risk Assessment Standard for Advanced Non-Light Water Reactors,” RA-S-1.4-2013, New York, NY (2013).